

Spatially localized microwave discharge in the atmosphere

V. A. Zhil'tsov, É. A. Manykin, E. A. Petrenko, and A. A. Skovoroda

Kurchatov Institute Russian Scientific Center, 123182 Moscow, Russia

J. F. Leitner

E.N.S.M., Aartselaar, B-2630 Belgium

P. H. Handel

University of Missouri, St. Louis, MO 63121

(Submitted 13 June 1995; resubmitted 26 July 1995)

Zh. Éksp. Teor. Fiz. **108**, 1966–1985 (December 1995)

A technique is described which ensures the production of spatially localized microwave discharges of spheroidal shape in the atmosphere, or "localized plasmas" (LP for short). Their basic properties are measured in various regimes: free movement in air; and steady-state in contact with a wall; and steady state away from walls. An analogy is established between the free movement of LPs in air and the movement of fireballs in the earth's atmosphere. The important role of laminar vortex motions inside LPs is pointed out; they are responsible for the shape and a certain amount of isolation of LPs from the surrounding space. The steady combustion state is described in general terms by the theory of equilibrium microwave discharges, taking into account the moderate motion of the gas due to convection. © 1995 American Institute of Physics.

1. INTRODUCTION

Steady discharges at atmospheric pressure have long been known. They have many applications in science and technology. Arc, rf, and microwave plasmatrons are widely used in plasma-chemical technologies.¹⁻³ Many present-day scientific instruments for analyzing materials contain such discharges.⁴ Suggestions for using microwave discharges to cleanse the atmosphere of freons are well known.⁵ Studies have also been carried out recently of the acoustic properties of microwave discharges in the atmosphere.⁶

It is customary to refer to the plasma in these discharges as low-temperature ($T < 1$ eV), and to describe it to lowest order using an equilibrium model (with the temperature of all the charged and neutral components approximately the same).⁷

Atmospheric discharges are generally structured. There are many studies of the different types of spatial structure at high microwave power density.^{8,9} For this reason electrodeless microwave discharges in the atmosphere offer an attractive possibility for explaining the natural phenomenon of ball lightning.¹⁰⁻¹⁴

In the present work spatially localized (with dimensions much less than the size of the discharge chamber) steady low-power microwave discharges of spheroidal shape have been studied both in an atmosphere which is at rest and in the presence of forced convection of the air. For the sake of brevity, we will call such a localized plasma an LP. We have posed the following problems: (a) to find a reliable way of producing LPs and (b) to study the physical properties and parameters of LPs at the lowest possible microwave power adequate for maintaining them in steady state. Unfortunately, the existing literature (see, e.g., Refs. 15–18) does not con-

tain adequate information about these questions, as far as we can tell.

In Sec. 2, we describe the experimental apparatus and the diagnostics employed. Section 3 is devoted to the analysis of different ways to initiate the discharge. In Sec. 4, the experimental results obtained from studying the properties of LPs are presented for various conditions: (a) free motion in the atmosphere; (b) LPs in contact with the chamber wall; and (c) in a configuration which is isolated from the walls by means of gas flows whose velocity is comparable with the velocity of free air convection in the discharge chamber. In Sec. 5 we discuss the experimental results, and in Sec. 6 we present conclusions.

2. EXPERIMENTAL APPARATUS

Figure 1 shows a schematic of the apparatus, which generally replicates the experiment of Ohtsuki and Ofurton.¹³ The magnetron had a fixed frequency of 2.45 GHz; the maximum power was 5 kW; the dimensions of the cylindrical copper chamber were 160 mm in diameter and 380 mm in length; a standard waveguide was connected to the copper chamber through a rectangular opening with dimensions 40×80 mm² located in the center of the chamber, with the smaller dimension in the direction of the chamber axis; the ends of the cylinder were closed with a woven brass grid with an opening size of 2×2 mm². In some of the experiments one of the grids was replaced by a movable metal piston. Several diagnostic ports were located in the midplane of the chamber.

Experiments revealed that precise determination of the physical parameters of an LP presents great difficulties. An LP is a complicated self-consistent object which entails the use of multiple diagnostics not only to measure the space and

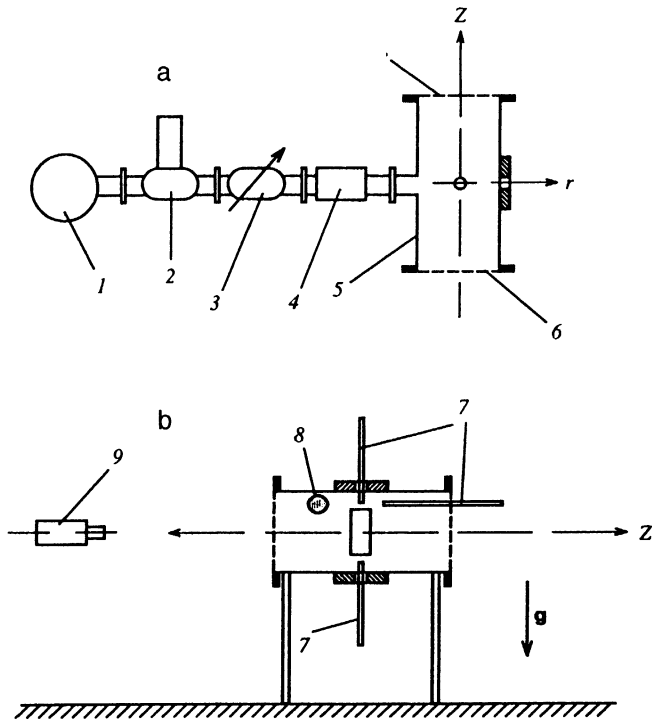


FIG. 1. Overall design of the apparatus: a) plan view; b) side view; 1) magnetron; 2) ferrite circulator; 3) gradual attenuator; 4) protective section; 5) discharge chamber; 6) end meshes. (b) Disposition of the cavity and diagnostics: 7) probe leads; 8) LP; 9) video camera (television camera, pyrometer, and monochromator).

time dependence of the plasma variables, but also for the spatial distribution of the microwave field intensity and the gas flow velocity in the discharge chamber and within the LP itself.

We used the following basic diagnostics:

- recording and subsequent processing of color video tapes with a frame rate of 50 Hz and minimum exposure of 1/8000 s;
- images of the LP recorded in the infrared region of the spectrum (3–7 μm) using a television camera;
- absolute measurements of the radiation losses in the 0.3–0.7 μm band using a radiometer;
- pyrometric and acoustic¹⁾ measurements of the LP temperature;
- calorimetric measurements of the power of the microwave generator, the power reflected from the discharge chamber, and the thermal power deposited in the walls of the discharge chamber;
- Langmuir “diving” probes thrust into the plasma for a short time (0.01–1 s) in order to keep them from being degraded;
- movable and fixed electromagnetic probes (loop antennas) to measure the distribution of the microwave field, including that within the plasma;
- optical spectra of the emission from the LP in the visible band.

3. INITIATION OF THE DISCHARGE

In order to produce a discharge in the atmosphere, it was first necessary to initiate it. This is related to the fact that the

electric field strength in the chamber prior to the onset of the discharge was much less than the breakdown strength of air at atmospheric pressure. The discharge chamber plays the role of an extra-large (dimension much greater than the wavelength of the microwaves) cavity facilitating the initiation of the LP. It is much easier to ignite the discharge when a single mode of oscillation is established in the discharge chamber prior to initiation by changing the size of the chamber. In the experiments we are describing here we used the mode TE_{214} .

We employed several methods for igniting the discharge, based on producing localized (within a small volume) conditions required for breakdown.

1. Introducing a flame (burning match, Bunsen burner, etc.) into the chamber. When this is done, the local heating of the air substantially reduces the gas density in the center of the flame, i.e., relaxes the breakdown condition.

2. Introducing a grounded metal needle into the chamber. When this is done, the strength of the microwave field at the needle increases and the heating due to the microwave fields lowers the gas density. This ultimately leads to a very efficient and simple way of initiating the discharge, the one we used most frequently.

3. Introducing an isolated metal tube of diameter 3 mm through which argon was fed at a low rate. When a spark breakdown was produced between the tube and the grounded discharge chamber, a plasmatron microwave discharge was ignited in the tube in the form of a jet which was then used to initiate the LP.

When a single mode of microwave oscillation was present in the discharge chamber, an initiator was placed at an antinode of the field, and the probability for initiating a discharge was essentially unity. This enabled us to perform measurements while the LP was moving upward, and not just in the steady state at the top of the wall (see below).

4. DISCHARGE PROPERTIES

4.1 Shape and time dependence of the discharge

Visual observation and analysis of the video tapes reveals the great variety of shapes in the discharge phenomena observed in the “geometry” of our experiments. Some of these were described in Ref. 13. Here we direct attention toward LPs of spherical shape in an atmosphere at rest and in the presence of forced convection of the gas in the chamber.

As an example, Fig. 2 shows the initiation of an LP in the center of the chamber using a plasmatron jet. The video frame was taken from the end of the chamber along its horizontal axis (see Fig. 1). The formation of an LP of spherical shape and its separation from the argon jet of the plasmatron can be seen. Note that the argon discharge is quenched after the LP separates from the tube. As shown by calorimetric measurements, this is associated with the fact that almost all the microwave power fed into the chamber was absorbed by the LP.

The buoyant (Archimedean) force caused by the reduction in the air density within an LP due to heating causes the LP to rise, and the diameter of the chamber determines the time of free flight (without wall contact). If the LP was ini-

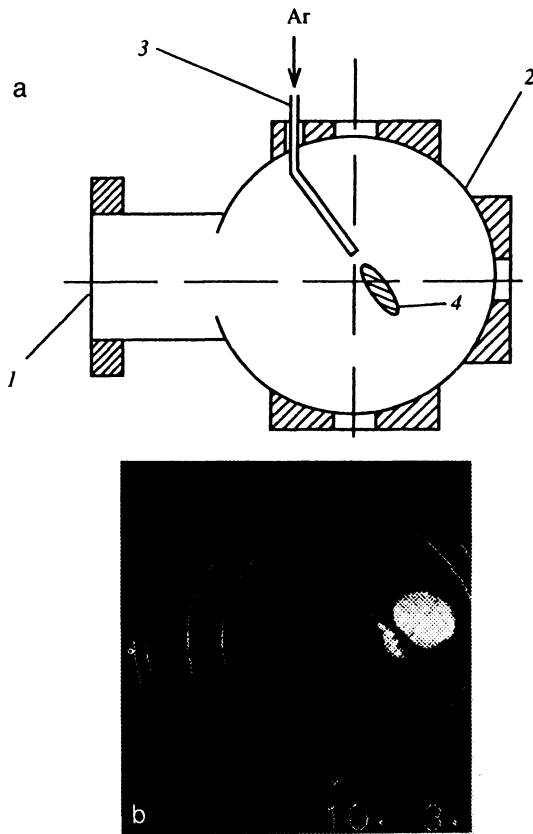


FIG. 2. a) Diagram of initiation using a plasmatron argon jet: 1) waveguide; 2) chamber; 3) copper tube for supplying argon; 4) jet. b) Video frame showing the formation of an LP using a plasmatron jet.

tiated at the bottom of the chamber, then it rose upward freely for 0.15 s until reaching the upper wall. Figure 3 shows the time dependence of the velocity with which the geometric center of the LP moves and the characteristic diameter during the rise. It is clear that the LP moves with an almost uniform velocity $v \approx 0.5$ m/s. The diameter of the LP increases from 4 cm at a rate $v_n \approx 0.1$ m/s. Note that in the free-ascent stage photographs with a short exposure time reveal no structures whatsoever other than spheroidal.

There are two different possibilities when the LP reaches the wall. If the microwave power fed into the chamber is less than 1.5 kW, then the LP is slowly quenched (this case is shown in Fig. 3). If the applied power is sufficiently high, then the LP, which assumes a hemispherical shape, remains stationary for many hours. Figure 4 shows a photo of stationary LP, demonstrating the existence of complex emission structure. The emission structure is found to be related to a spot on the metal wall in the center of the LP. This spot always appears when the LP approaches a metal surface to within 5 mm and disappears when the LP is pulled away from the wall as a result of forced convection of the air (see below) or by using an auxiliary insulating (quartz) upper wall in the discharge chamber. We associate this spot with the appearance of an arc due to the detecting properties of a microwave discharge at a metal wall.¹⁹

This behavior of the LP is typical. In some cases it is possible to briefly observe the simultaneous existence of two or more LPs. Under steady-state conditions with a metal up-

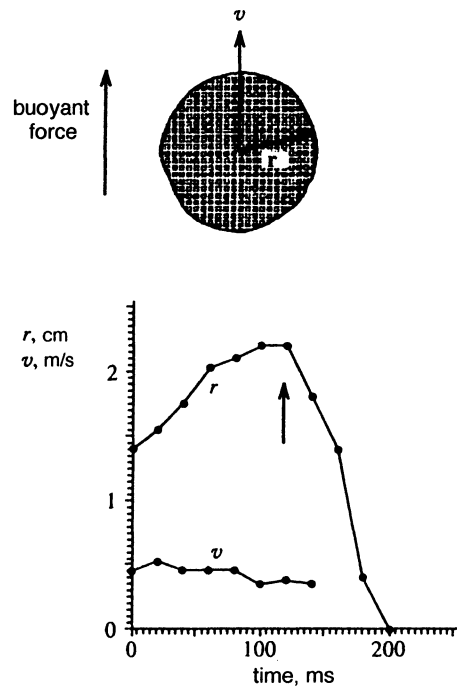


FIG. 3. Dependence of the radius r and spreading velocity v in an LP in flight. The arrow indicates the time at which the LP touches the chamber wall.

per wall a single LP is always observed. Under steady conditions with an insulating wall two or more LPs are seen, depending on the microwave power (the number of separate LPs increases with power).

Measurements are described of the LP parameters under typical steady conditions at the wall (metal or insulation). We also measured the LP variables in the state isolated from the wall. This time-dependent state exists while the LP is moving within the chamber. It is possible to produce a stationary state with an LP isolated at a fixed point in the chamber by employing forced convection of the air within the chamber.

4.2 Parameters of an LP in contact with the wall

a. *Energetic properties.* Calorimetric measurements of the power P_{gen} of the microwave generator, the reflected microwave power P_{ref} , and the thermal power P_{hp} deposited in the walls of the discharge chamber confirmed the relation

$$P_{\text{gen}} = P_{\text{ref}} + P_{\text{hp}}. \quad (1)$$

This allows us to treat P_{hp} as the LP power, equal to ~ 1.5 kW for the present experiments. We recall that if the magnetron power is reduced below this level the LP exists in a state of motion, but vanishes when it comes in contact with the wall. As the power increases, the size of a steady LP increases slightly. The validity of Eq. (1) and direct measurements show that the radiation losses of the LP are negligible in comparison with the thermal conduction and convection losses to the wall of the discharge chamber.

b. *Measurement of the gas temperature within the LP.* When probes and tungsten filaments were inserted into the center of the LP they melted and vaporized, which shows that the gas temperature T is about 3000 K. Pyrometric mea-

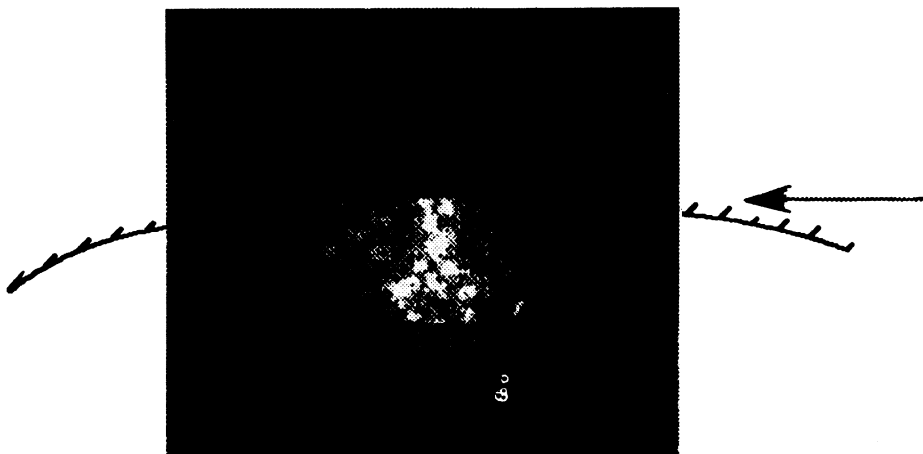


FIG. 4. Video image of an LP located at a fixed point near the wall of the cavity. The arrow indicates the top of the chamber.

measurements yielded a temperature $T=3500\pm 500$ K, which is close to that found in other experiments and calculations.^{5,18}

The spatial temperature distribution was determined by means of infrared television imaging. Figure 5 shows infrared and visible images of a stationary LP (the exposure time for a photo in the visible is considerably longer than that in the photograph of Fig. 4, so that the image is "burned in" in comparison with the infrared image). Their spheroidal shape, the approximate equality of the dimensions, and the presence of a hot core can be seen. Color video images of the LP reveal that the colors vary from the center to the periphery, which confirms the existence of a hot center and a fairly abrupt drop in temperature at the periphery. Note that, as shown by infrared measurements, when the LP is moving the center has a higher temperature than after contact with the wall.

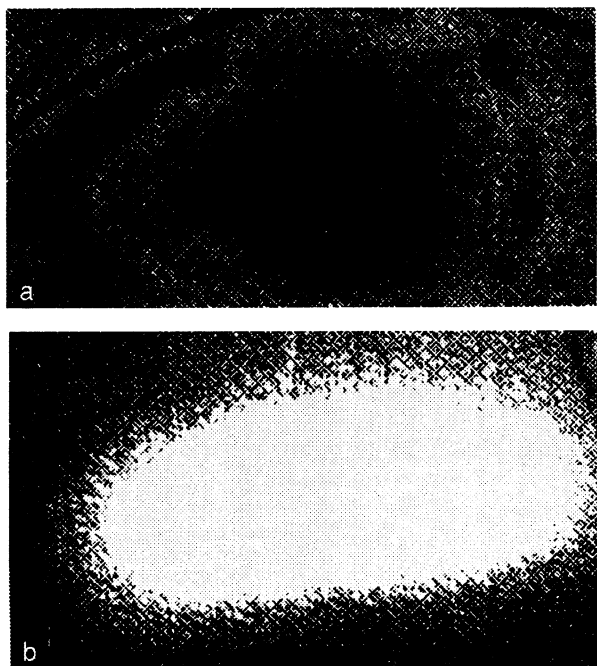


FIG. 5. Video images of an LP in the infrared (a) and optical (b) spectral bands.

The distributions shown in Fig. 5 have an integrated character, since the intensity of the recorded emission depends on the size of the radiating region in the direction of the shot. The photos reveal that the integrated intensity varies with radius quite smoothly in the center, which does not rule out the possibility of a dip in the temperature profile in the center.

c. Optical spectral measurements. Line-of-sight spectra were measured in the visible band. The spectra are continuous; they exhibit the molecular bands of the components of air and are characterized by the absence of intense lines for single atoms. The nature of the spectrum corresponds to the measured gas temperature. Note that when additional argon is injected into the chamber the nature of the spectrum changed little, and practically no individual argon lines were detected. The general nature of the spectrum was close to those of hot flames in combustion.²⁰

d. Probe measurements. Prolonged insertion of fine probes within the discharge chamber is impossible because they burn up when microwave power is applied. However, if we insert a probe quickly parallel to the wall of the discharge chamber, it is not destroyed and can pass through the plasma. We used an ordinary Langmuir probe in order to measure the electron temperature and density and the plasma potential,⁷ and electromagnetic probes to measure the distribution of the microwave fields in the discharge chamber and within the LP.

The measurements showed that the LP has a positive potential of a few volts in contact with the metal wall. When the LP was on an insulating wall, its potential dropped by two orders of magnitude and was equal to 0.05–0.07 V.

When an LP is present, the structure of the microwave fields in the chamber undergoes a fundamental change in comparison with that of the TE_{214} mode which is present prior to breakdown. The LP parameters in steady state are practically independent of variation in the discharge chamber geometry (changing its size by means of the movable piston, opening orifices of diameter 100 mm). If a movable horizontal quartz partition is inserted into the chamber, the LP can be fixed to this partition (wall) at any point of the chamber, including its center. The strength of the microwave fields in the chamber is greatest at the surface of the LP and falls off

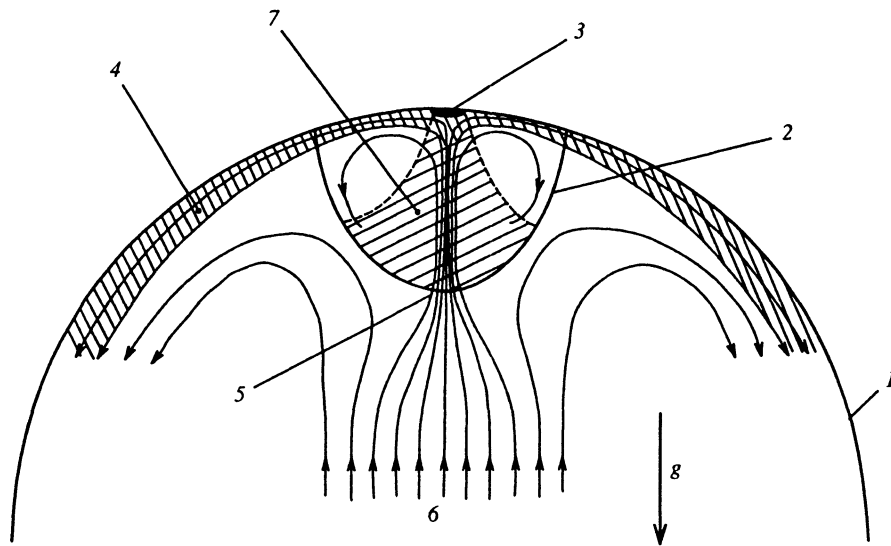


FIG. 6. Diagram of the gas circulation near an LP: 1) chamber wall; 2) visible plasma boundary; 3) bright spot; 4) streamlines of the hot air; 5) region where the cold gas is fed in; 6) flow of cold air; 7) region of brightest emission. Here g is the vector gravitational acceleration.

toward the center of the LP with a characteristic gradient $\sim 1 \text{ cm}^{-1}$. The distribution of the microwave fields in the discharge chamber outside the LP was also measured using the television camera. For this purpose a sheet of Whatman paper was placed in the chamber and the distribution of the thermal fields was recorded on it; this is unambiguously related to the distribution of the microwave electric field.

e. *Structure of the free convective gas flows.* The time-independent state of free (spontaneous) convection was studied at a metal wall. The gas flow outside the LP was visualized by means of video tapes of thin smoke trails. We succeeded in visualizing the gas flow along the trajectories of small luminous particles within the LP produced by placing a thin ceramic rod at the boundary of the LP and vaporizing it. Figure 6 shows the flow pattern reconstructed from these measurements.

The most distinctive feature of this flow is the presence of a singular point with zero velocity. The position of this point coincides with the luminous spot (Figs. 4 and 6). Cold gas at room temperature T_{room} enters primarily at the center of the LP, increasing abruptly in velocity (by a factor T/T_{room}), and heat is deposited by the hot air from the LP over the walls of the discharge chamber. These flows of hot air are clearly visible in the infrared images of the discharge. The gas velocity within the LP is about 0.3 m/s.

From Fig. 6 it is clear that the LP has a tendency to develop a laminar vortex structure (in the form of a Hill's vortex²¹). We did not entirely succeed in imaging the vortex, since the fine ceramic particles either burned up rapidly or ceased to glow in the colder regions at the periphery of the LP. In order to convince ourselves indirectly of the presence of the vortex structures inside the LP we performed an experiment in which the solid upper wall of the chamber was replaced by a mesh. When this was done, the structure of the microwave fields did not change, but the convective flow of hot air was able to pass freely upward. The experiment showed that the change in the wall had no effect on the shape or nature of the discharge. The spot formed at one of the sectors of the mesh, and the lifetime of the LP (several minutes) was determined by the degradation of the mesh at this

spot. The persistence of the shape of the LP when the nature of the convection underwent a qualitative change clearly shows, in our opinion, that a vortex is present within the LP (see also below).

An attempt was made to pull the LP away from the solid chamber wall by pumping out the gas. For this purpose a quartz tube of diameter 20 mm was brought up to the stationary LP from below. It was connected to the exhaust system and the gas flow rate was adjusted. Even when air was pumped out through the tube at a high rate the LP failed to separate from the wall, but a long thin filament reached into the tube, as shown schematically in Fig. 7. The situation did not change when an insulating wall was used for the upper part of the discharge chamber.

f. *Decay of the LP.* When the microwave power was shut off rapidly (over $\sim 2 \mu\text{s}$) the visible emission of the plasma stopped fairly gradually. Figure 8 shows an oscilloscope trace of the emission intensity when the LP was decaying at the chamber wall. The decay obeys an exponential law with a time constant of 10 ms.

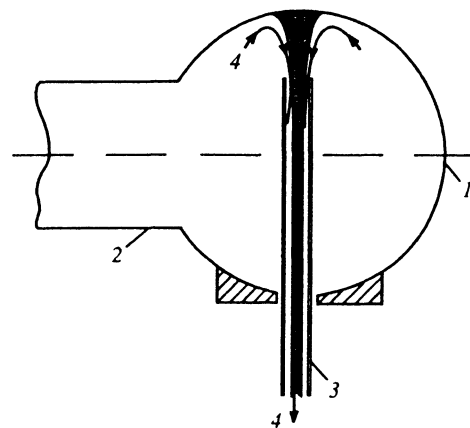


FIG. 7. Diagram of the behavior of an LP in contact with the wall when gas is pumped out of the cavity (view from the chamber endwall); 1) chamber; 2) waveguide; 3) quartz tube through which the air is pumped out; 4) gas streamlines. The radiating region is shown darker.

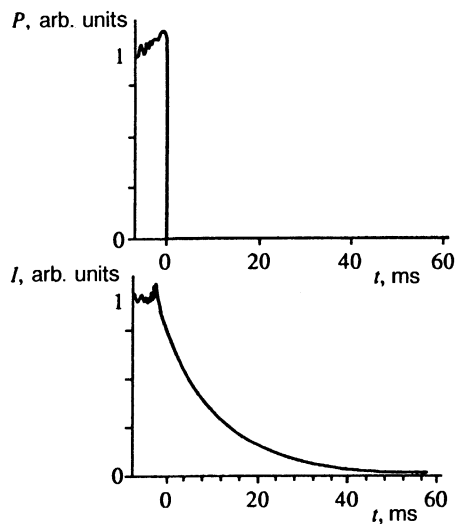


FIG. 8. Oscilloscope trace of the emission from an LP at the wall after the magnetron is switched off: P is the detected signal from a microwave antenna in the chamber and I is the current from the photomultiplier tube which detects the LP emission in the visible region.

Table I gives typical values of the parameters of an LP at the wall.

4.3. Isolated state of the LP

A time-dependent isolated state of the LP was attained in the free-flight stage following discharge initiation (Figs. 1 and 2). The values of the LP variables measured in this state are shown in the table for a fairly high power input into the chamber, which is required for reliable breakdown. This power is not the smallest value needed to maintain the discharge during motion. Note that the time for the LP emission to be extinguished after the microwave generator is shut off abruptly at the start of motion is considerably longer (0.1 s) and is limited by the time of flight across the chamber.

Two ways to produce stationary isolated states using forced air convection were studied. In the first approach, after a steady state with the LP at the wall was established in an atmosphere at rest, specially designed nozzles produced an intense azimuthal circulation of air about the discharge chamber axis (the end walls of the discharge chamber do not affect the gas flow, since they are made of mesh). The LP is

pulled away from the walls and displaced toward the axis, exhibiting a complicated motion and distortion of its shape. Most of the time a single LP decayed into two, which display a coupled rotational motion about the axis of the cylinder. Figure 9 shows several successive frames of video tape with a short exposure time under these conditions. We were unable to make the discharge stop at a particular point in space.

In the second approach forced air convection in the chamber was used to position a spheroidal LP in the center of the chamber, isolated from the walls, with air being supplied at a low rate (<0.1 l/s). Figure 10 shows the design of the experiment and a photo of the LP in the chamber. A length of quartz tube of large diameter was placed at the center of the chamber. Air was pumped down the tube along the axis in a controlled fashion through a hole in the wall of the chamber. After the LP was initiated it remained fixed close to the upper end of the tube, separated from the chamber wall and the quartz tube. The distance by which the LP penetrated into the tube was adjusted via the rate at which air was pumped out and by changing the size of the tube. In the experiments we used quartz tubes of diameter 70–90 mm and length 90–120 mm. When the LP was partly inserted into the tube we measured its parameters using the diagnostics described above. The results of these measurements are shown in the table.

In comparison with the case when the LP was at the wall, less power was needed to maintain it in the isolated state. This is because of the reduction in heat losses in the isolated state. The lowest LP temperature shown in the table was found in just this state.

Optical spectra of the emission from an LP associated with azimuthal circulation and in the isolated state are similar to the spectrum of an LP on the wall. We note, however, that in the isolated state an LP at low temperature does not exhibit the characteristic cyan lines.

When thin ceramic probes were vaporized we were able to track the structure of the gas flows within the LP and found closed circulating flows (vortices). The typical velocity of the gas in the vortices was 0.2 m/s.

5. DISCUSSION

Let us estimate some parameters of an LP in steady state at the wall according to the theory of equilibrium microwave discharges,^{7,16,17} using the concept of the normal propagation

TABLE I. Typical LP parameters.

Type of LP	at wall	free motion	isolated
Microwave power absorbed in the LP for stable burning, kW	1.5	1.5	0.5
LP radius, cm	2	1–3	3
Microwave intensity, W/cm ²	50	-	5
Specific absorbed power, W/cm ³	50	-	5
Temperature, K	3500 ± 500	4000	2500
Characteristic gas velocity inside the LP, m/s	0.3	0.5	0.2
Characteristic rate at which the LP expands, m/s		0.1	
Plasma density, cm ⁻³	10 ¹³	-	2 · 10 ¹²
Skin depth, cm	1–1.5	-	2–3
LP potential relative to the chamber, V	+5	-	+0.06
Decay time, s	0.01	0.1	≥ 0.15

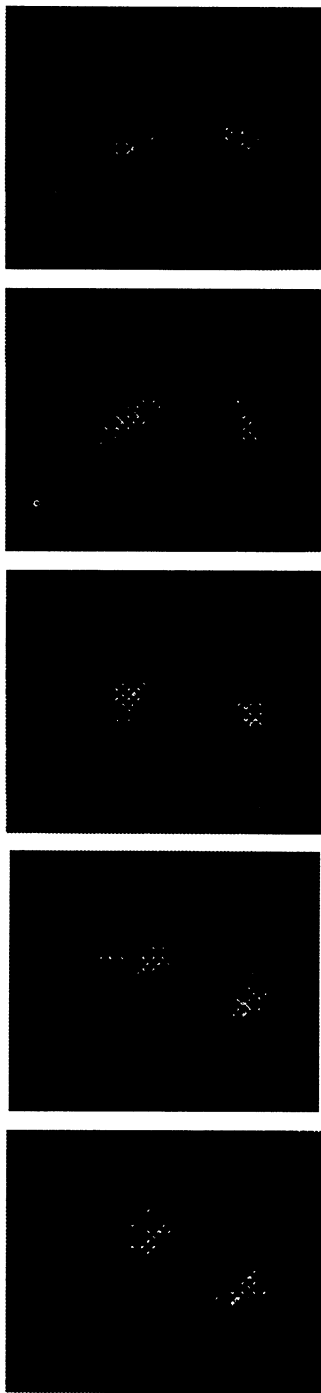


FIG. 9. Video frames of an LP with induced azimuthal gas circulation. The time between frames is 20 ms.

velocity v_n of an ionization front, analogous to the well-known flame propagation speed.²² The ionization front propagates down from the wall, while the convective air flows rise upward in the opposite direction. Using the analog of the Zel'dovich formula⁷

$$v_n = S_0 / \rho_0 w(T), \quad (2)$$

where S_0 is the microwave intensity at the LP, ρ_0 is the density of cold air, and w is the specific enthalpy of the heated air, and substituting into it the measured values of the

parameters, we find that v_n has a value close to 0.1 m/s. The gas inside the LP moves with approximately this velocity, which accounts for the stationary boundary of the LP.⁷ We can take into account the mechanism of microwave heating of the LP in a skin layer at the boundary explicitly and find the following expression:⁷

$$v_n = \frac{\chi}{\delta} \frac{4kT}{I} \frac{c_p T}{w} \frac{\rho}{\rho_0}, \quad (3)$$

where χ is the thermal conductivity of the hot air, δ is the skin depth, c_p and ρ are the specific heat and density of the hot air, and I is the effective ionization potential. Substituting the measured speed of the gas in the LP and the skin depth δ , we obtain a gas temperature T close to the measured value. Note that the characteristic size of the LP is close to the skin depth. It is precisely this case which gives rise to the most effective heating of the entire volume of the LP by absorption of the microwave currents in the skin layer. The cooling of the LP after the heating source is turned off is determined by the convective and conductive heat efflux, and a rough estimate shows it to be close to the measured time for the extinction of the LP emission.

When the microwave power is reduced below some threshold value the discharge disappears (the table gives values close to the threshold value). This is also in qualitative accord with theory. However, numerical calculation of the threshold power depends sensitively on the shape of the discharge, and it can be predicted by equilibrium theory only to order of magnitude.

Thus, the existing theory enables us to explain the main quantities of a time-independent LP at the upper wall in general fashion.

However, thus far we have assumed that the nature of the gas flow is actually known, whereas in the experiment it is determined by free convection induced by inertial forces and the temperature gradient, i.e., it must be evaluated self-consistently with the discharge. The decisive role of free convection on the properties of discharges in the atmosphere was beautifully demonstrated in experiments²³ with freely falling arcs, where the force of gravity was absent. Note that existing theoretical models generally assume only irrotational motion of the gas in the hot core of the discharge, while the present experiments imply that laminar rotational structures form in the LP even when it is at the wall.¹⁸

Existing theoretical concepts may also qualitatively explain our experiments with forced convection. Specifically, the time independence of the ionization front requires that the gas velocity equal the propagation speed of this front. Hence the microwave discharge should be localized around a singular region where the gas velocity is low (vanishes), and consequently a spatial gradient of the velocities exists which guarantees that the condition for the front to be stationary holds.³ In the presence of forced circulation such regions developed in the center of individual vortices or on the axis of the cylindrical chamber, where the LP is in fact observed experimentally. When forced convection is established at the wall by exhausting air through a narrow tube of diameter 1–2 cm (see Fig. 7), a singular region with zero velocity is maintained at the metal surface for arbitrary exhaust rates.

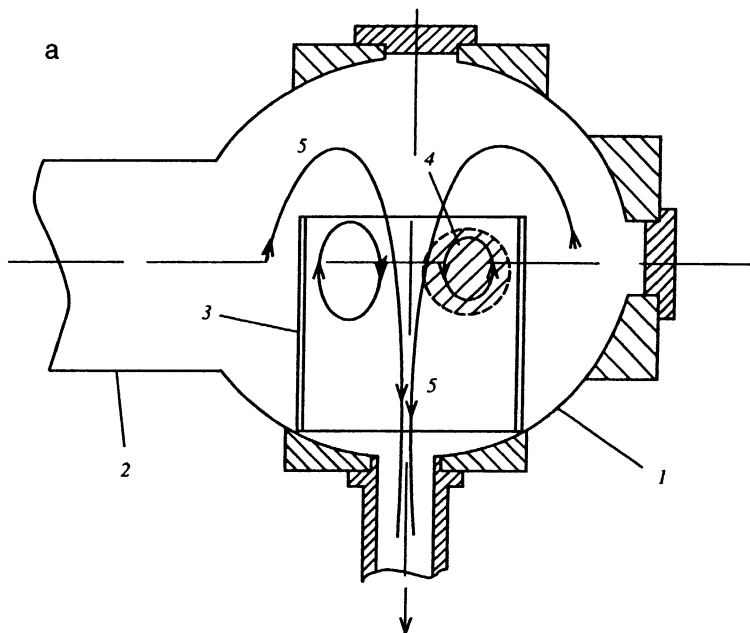
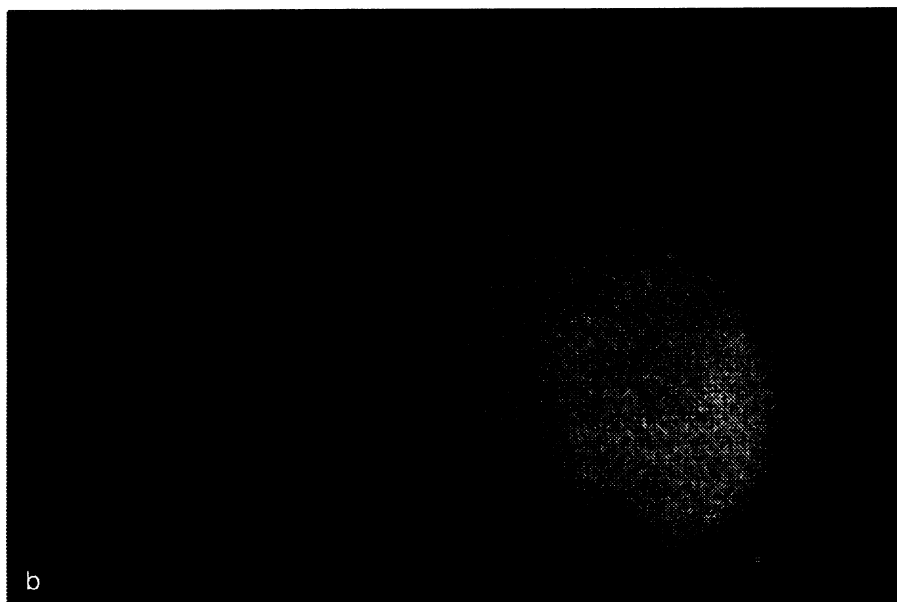


FIG. 10. a) Diagram of the creation of an isolated LP state: 1) chamber, 2) waveguide; 3) quartz tube; 4) LP; 5) gas streamlines. The arrow indicates the direction in which gas was exhausted from the chamber. The tube diameter was 90 mm and its length was 120 mm; the wall thickness was 1 mm. b) Video image of an isolated LP.



This is the explanation for the impossibility of pulling the LP away from the wall and for the shape of the plasma burning in this experiment.

When wide quartz tubes (with diameter 8–10 cm) which are sufficiently short (separated from the upper wall) are used with a low air exhaust rate (Fig. 10), a rotational region (where the air stagnates) forms alongside the upper edge of the tube. That is where the LP is localized. Cold air is pumped down through the tube from the entire interior of the chamber. Hot air near the LP rises up along the hot walls of the tube. A vortex motion develops, in the center of which the LP is located. When this happens the LP is observed either on the near edge of the tube, close to the waveguide bringing in the microwaves, or on the far edge. By carefully symmetrizing the air flows in the tube we were able to create

two LPs simultaneously and to observe the air circulating in opposite directions in these LPs.

Note that to isolate the LP it is necessary to pump air out, not in, since this gives rise to instability in the isolated state even for arbitrarily low air flow rates. The forced motion of the air in this experiment is of the same magnitude as the induced free convection. In fact, the forced air motion balances the buoyant force.

In this connection the most interesting question becomes that of the structure of the gas flow in the free-flight stage of the LP, when the spheroid is surrounded by an atmosphere at rest. This question is closely related to the problem of describing the uniform motion of the LP observed experimentally and explaining the spherical shape of a free LP.

We note that there is practically no theory for the motion

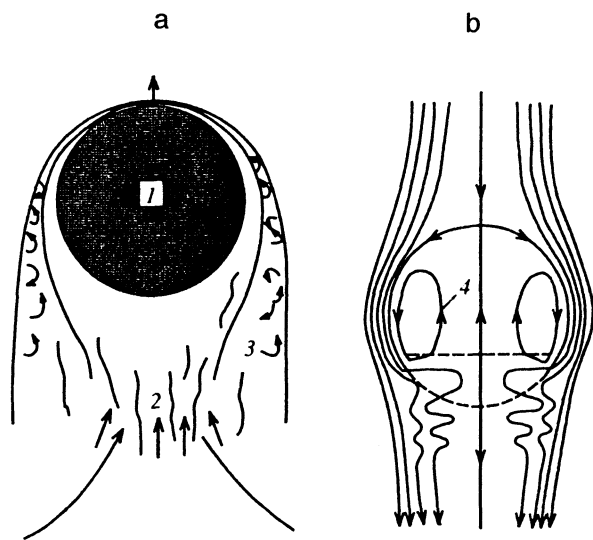


FIG. 11. Structure of the gas flow in a fireball. a) Diagram of the motion of the locally heated air volume due to the buoyant force. b) Air streamlines associated with the rise of the fireball in the atmosphere: 1) heated air mass; 2) wake; the arrow shows the direction in which air flows into the wake; 3) transitional air; 4) Hill's vortex.

of discharges, in particular LPs, in the atmosphere. For example, there is no unique answer to the question of whether a solid-state description for the motion of an arc in the atmosphere is possible.²⁴ Probably the closest physical analog of the LP in these experiments is a "fireball."²⁵ A fireball is a physical phenomenon, consisting of a local spheroidal region of elevated temperatures in the earth's atmosphere, arising spontaneously or as a result of a (nuclear) air blast. Figure 11 shows the structure of the gas flow in a fireball which is accepted at the present time. The buoyant motion of a fireball upward from the earth's surface is described by the following equation:

$$v = g \frac{T - T_{\text{room}}}{T_{\text{room}}} - \frac{3}{8} \left(\frac{3}{2} K + \xi \right) \frac{v^2}{R}, \quad (4)$$

where R is the LP radius, ξ is the drag coefficient, K is the fraction of the fireball mass involved in the exchange with the surrounding atmosphere, and g is the gravitational acceleration.²⁵ In this equation the first term on the right-hand side describes the buoyant force, the second term is the gas flow through the fireball, and the third term is the turbulent drag. The viscous drag (the Stokes force) is dropped because it is small in comparison with the buoyant force. The uniform motion of the LP fireball in our experiment ($v=0$) can be explained only by the turbulent drag resulting from gas flow through the LP. Specifically, hot air in the center of the LP rises, so that the upper boundary pushes the denser motionless cold air aside and entrains it in the rarefaction region that develops in the wake. Vorticity is created there which slows down the motion of the LP (Fig. 11a). This picture of the motion is tenable only if there is some mechanism which preserves the spheroidal shape of the LP in the course of the motion. In an atmospheric fireball the formation of a Hill's vortex²¹ in the "head" of the fireball serves as

this mechanism²⁵ (Fig. 11b). A similar mechanism probably also pertains to the case of a stationary isolated LP.

Evidence that such a mechanism acts in the case of the LP comes from the following experimental facts:

1) The LP rises at a uniform rate, maintaining its spherical shape. Equation (4) yields a constant value equal to 0.5 m/s for the upward velocity of the LP if we use the turbulent drag for a solid sphere of radius 2 cm with a Reynolds number of 2500 and assume that the fractional gas exchange is $\approx 50\%$.

2) Laminar rotational motions of the gas inside the LP are observed with the characteristic dimensions of the LP and velocities on the order of that of the LP as a whole.

3) The shape of the LP at the wall does not depend on whether the wall is solid or a mesh.

4) Cold air enters an LP at a wall in a narrow central channel underneath the LP.

5) The core of the LP is isolated to a certain extent from the surrounding medium. When a radiating impurity such as the salt NaCl is introduced rapidly into the interior of the LP, the characteristic yellow Na line is observed for a considerable time (several seconds). When argon is admitted outside the LP and Ar line is not observed in the optical spectrum. Note that microwave discharges in the atmosphere exhibit a certain amount of chemical isolation in experiments and in calculations performed in connection with plasmatron work.^{3,18}

It should be pointed out that the isolation of the LP may also be connected with the fact that in a low-temperature plasma formed in atmospheric gas there is a quite substantial concentration not only of neutral atoms in the ground state but also of highly excited Rydberg states (with large quantum numbers $n \sim 10$). In the appendix we discuss this question further.

Now we will discuss the presence in a stationary LP at a metal wall of a potential substantially higher than the measured electron temperature, which somewhat exceeds the gas temperature. We link the appearance of this potential with the occurrence of the arc spot, which is characteristic of a stationary LP at a metal surface. The spot always appears when the LP approaches a metal surface, which evidently occurred in the experiments with forced circulation, when a change in the rate at which air was supplied to the nozzles producing the circulation resulted in a change in the distance between the LP and the wall. Sometimes not one but two parts of the plasma approached the wall when the vortex shape of the LP was complicated, and each approach gave rise to a spot. The potential arises as a result of the detection of a microwave field in a nonlinear metal-plasma junction,¹⁹ and its large value is related to the large value of the microwave field strength in the discharge chamber. Note that, as can be seen from Figs. 4 and 6, where a spot is present there is an additional bright emission superposed on the usual emission from the LP having a spheroidal shape. This additional emission comes from the spot and spreads out like a fan as it moves down from the wall. The infrared picture (Fig. 5) exhibits a featureless spheroidal shape associated with the spot. We have found no explanation for this phenomenon.

6. CONCLUSION

These experiments enabled us to exhibit the conditions for LPs to exist in isolation and interacting with metal and insulating walls, and to determine their parameters. The structure of the microwave fields in a discharge chamber undergoes a fundamental change when LPs develop. The use of gas flows or insulating walls permits LPs to be positioned at an arbitrary point in the discharge chamber. The experiments imply that laminar rotational gas flows have a decisive effect on the shape and on the values of the variables in an LP. This is seen most clearly when LPs move freely in an atmosphere at rest, so that the motion of the LP closely resembles that of a solid sphere. Note that the simple technique employed here, which guarantees that LPs are produced for arbitrarily low power fluxes, enables us to model a number of plasma, plasma-chemical, and gas dynamic processes in the atmosphere.

We thank A. V. Timofeev for his interest in this work and for discussing it.

APPENDIX

To estimate the relative numbers of atomic states in a gas we calculate the statistical weights for hydrogenlike atoms, following the familiar procedure of statistical physics. In our case the total statistical sum is given by the formula (see, e.g., Ref. 26)

$$Z = \sum_{n=1}^{\infty} 2n^2 \exp(-\beta E_n) + Z_p = Z_n + Z_p, \quad (\text{A1})$$

where we have written $E_n = R - R/n^2$, $\beta = 1/kT$, and $R = me^4/2\hbar$ is the Rydberg constant. The n summation is over discrete states, and for the continuous spectrum we have

$$Z_p = \int \frac{d^3p d^3x}{(2\pi\hbar)^3} \exp\left\{-\beta\left(R + \frac{p^2}{2m}\right)\right\}. \quad (\text{A2})$$

In the general case the first term in (A1) diverges. This well-known paradox is related to the use of an infinite volume. For a bounded volume the sum must be "cut off" at some value of n . We will proceed from the fact that the size of a highly excited atom must be less than some characteristic volume V . Retaining a finite number of terms in Z_n we find

$$Z_n = 2 + 8 \exp\left\{-\frac{3}{4}\beta R\right\} + \dots + 2N^2 \exp\{-\beta E_N\}. \quad (\text{A3})$$

Starting at some $n = n_0 < N$ we have $E_n \sim R$. Hence the contribution to Z_n of the remainder $Q(n_0 < n < N)$ can be evaluated by transforming from summation to integration:

$$Q = 2e^{-\beta R} \int_{x_0}^{X^{1/2}} dx \frac{x^2}{a_0^3} \sim e^{-\beta R} \left(\frac{X}{a_0}\right)^{3/2}. \quad (\text{A4})$$

Here $a_0 = \hbar^2/me$ is the Bohr radius, and we have written $x_0 = n_0^2 a_0$ and $X = N^2 a_0$ and assumed $x_0 \ll X$. Note that $4\pi X^3/3 = V$ is the volume occupied by a Rydberg atom with $n = N$. Thus, we see that $Q \sim \sqrt{V}$.

The quantity Z_p is evaluated by the familiar technique of integration over a finite volume V :

$$Z_p = 2\pi^{3/2} e^{-\beta R} \frac{V}{\lambda^3} \sim e^{-\beta R} \left(\frac{X}{\lambda}\right)^3, \quad (\text{A5})$$

where $\lambda = 2\pi\hbar/\sqrt{2mkT}$ is the de Broglie wavelength.

At atmospheric pressure and a temperature $T \sim 3000^\circ\text{C}$ the density of neutral atoms in the ground state is $N_0 \sim 3 \cdot 10^{18} \text{ cm}^{-3}$. The free volume associated with a single atom is $V \sim N_0^{-1} \sim 10^{-18} \text{ cm}^{-3}$, i.e., $X \sim 10^{-6} \text{ cm}$. For thermal electrons at the specified temperature we obtain $\lambda \sim 2 \cdot 10^{-7} \text{ cm}$, i.e., $(X/\lambda)^3 \sim 10^3/8$. This implies $(X/a_0)^{3/2} \sim 10^3$ ($n \sim 10$). From these estimates it follows that the degree of excitation to levels $n \sim 10$ and the degree of ionization are almost identical, and the corresponding densities are $10^{13} - 10^{14} \text{ cm}^{-3}$.

Air molecules in Rydberg states are subject to a strong van der Waals attraction, which can cause a condensed state to form from excited systems.²⁷⁻²⁹ This may have a considerable effect on all the properties of the LP, both aerodynamic and optical.

¹The temperature was measured from the change in the velocity of an ultrasound wave passing through the LP (40–80 Hz).

¹A. S. Karoteev, V. M. Mironov, and Yu. S. Svarchuk, *Plasmatrons* [in Russian], Mashinostroenie, Moscow (1993).

²S. V. Dresvin, *Introduction to the Theory and Calculation of High-Frequency Plasmatrons* [in Russian], Énergoatomizdat, Leningrad (1991).

³*Low-Temperature Plasma; Rf and Microwave Plasmatrons* [in Russian], Nauka, Novosibirsk (1992).

⁴R. Baffington, *Use of Atomic-Emission Spectroscopy in High-Frequency Discharges for Gas Chromatography* [Russian trans.], Mir, Moscow (1994).

⁵G. A. Askar'yan, G. M. Batanov, S. I. Gritsinin *et al.*, in *Int. Workshop, Microwave Plasma and Its Applications*, Zvenigorod, Russia, Sept. 5–8, 1994.

⁶V. A. Zhil'tsov, A. A. Skovoroda, and A. V. Timofeev, *Zh. Éksp. Teor. Fiz.* **106**, 1687 (1994) [*Sov. Phys. JETP* **79**, 912 (1994)].

⁷Yu. P. Raizer, *Discharge Physics*, Springer, New York (1991).

⁸V. G. Brovkin and Yu. F. Kolesnichenko, in *Int. Workshop, Microwave Plasma and Its Applications*, Zvenigorod, Russia, Sept. 5–8, 1994.

⁹A. L. Vikharev, O. A. Ivanov, and A. G. Litvak, in *Int. Workshop, Microwave Plasma and Its Applications*, Zvenigorod, Russia, Sept. 5–8, 1994.

¹⁰P. L. Kapitsa, *Dokl. Akad. Nauk SSSR* **101**, 245 (1955); *Zh. Éksp. Teor. Fiz.* **57**, 1801 (1969) [*Sov. Phys. JETP* **30**, 973 (1970)].

¹¹J. R. Powell and D. Finkelstein, *Amer. Sci.* **58**, 262 (1970) [cf. J. D. Barry, *Ball Lightning and Bead Lightning*, Plenum, New York (1980)].

¹²P. H. Handel, in *Science of Ball Lightning (Fireball)*, Y. Ohtsuki (ed.), World Scientific, Singapore (1989).

¹³Y. H. Ohtsuki and H. Ofurton, *Nature* **350**, 139 (1991).

¹⁴*Ball Lightning in the Laboratory* [in Russian], Khimiya, Moscow (1994).

¹⁵Yu. P. Raizer, *Laser-Induced Discharge Phenomena*, Consultants Bureau, New York (1977).

¹⁶Yu. P. Raizer, *Foundations of the Modern Physics of Gas-Discharge Phenomena* [in Russian], Nauka, Moscow (1980).

¹⁷S. V. Dresvin (ed.), *Introduction to the Theory and Technique of High-Frequency Plasmas* [in Russian], Atomizdat, Moscow (1980).

¹⁸V. M. Lelevkin and D. K. Otorbaev, *Physics of Nonequilibrium Plasmas*, North-Holland, Amsterdam (1992).

¹⁹K. I. Kononenko, *Detection Properties of Gas-Discharge Plasmas* [in Russian], Atomizdat, Moscow (1980).

²⁰V. A. Kamanshikov, Yu. A. Platinin *et al.*, *Radiation Properties of Gases at High Temperatures* [in Russian], Mashinostroenie, Moscow (1971).

²¹H. Lamb, *Hydrodynamics*, 6th ed., University Press, Cambridge (1932).

²²Ya. B. Zel'dovich, G. I. Barenblatt, V. B. Librovich, and G. M. Makhviladze, *The Mathematical Theory of Combustion and Explosions*, Consultants Bureau, New York (1985).

²³M. Steenbeck, *Phys. Z.* **38**, 1099 (1937). (cf. V. Finkelnburg and H. Mecker, *Electron Arcs and Thermal Plasmas* [Russian translation], IL, Moscow (1961)).

- ²⁴“Low-Temperature Plasma,” in *Theory of the Electric Arc Column* [in Russian], Nauka, Novosibirsk (1991).
- ²⁵N. K. Vinnichenko, N. Z. Pinus *et al.*, *Turbulence in the Free Atmosphere* Consultants Bureau, New York (1980).
- ²⁶L. D. Landau and E. M. Lifshitz, *Statistical Physics, Part I*, Pergamon, Oxford (1980).
- ²⁷É. A. Manykin, M. I. Ozhovan, and P. P. Poluéktov, Dokl. Akad. Nauk

- SSSR 260, 1096 (1981) [Sov. Phys. Dokl. 26, 979 (1981)].
- ²⁸É. A. Manykin, M. I. Ozhovan, and P. P. Poluéktov, Zh. Éksp. Teor. Fiz. 84, 442 (1983) [Sov. Phys. JETP 57, 256 (1983)].
- ²⁹É. A. Manykin, M. I. Ozhovan, and P. P. Poluéktov, Zh. Éksp. Teor. Fiz. 102, 1109 (1992) [Sov. Phys. JETP 75, 602 (1992)].

Translated by David L. Book